

Performance Improvement of Indium Tin Oxide Electrochemical Sensor by Mixing Carbon Black

Changhan Lee,¹ Sangsu An,¹ Youngji Cho,¹
Jiho Chang,^{1*} Jaejin Park,² and Moonjin Lee²

¹Major of Nano-semiconductor Engineering, Korea Maritime & Ocean University, Busan 49112, Korea

²Ocean and Maritime Digital Technology Research Division, Korea Research Institute of Ships and Ocean Engineering, Daejeon 34103, Korea

(Received March 15, 2024; accepted May 1, 2024)

Keywords: hazardous substances in water, ITO, carbon black, morphology, sensor

We studied a method of implementing an electrochemical sensor with high response speed using a film made of metal oxide nanoparticles. The optimal conditions for sensor production were estimated by calculating the sensor's response when the bulk and surface resistances of the film changed. We also implemented a new manufacturing process to fabricate the sensor. To achieve high response speed, an ITO:CB film was produced by mixing ITO nanoparticles and carbon black (CB) powder. Depending on the CB content of the ITO:CB film, the response time of the sensor continued to decrease from 337 s (CB = 0 wt%) to 2 s (CB = 50 wt%). However, even in this case, a continuous decrease in response intensity was observed as well. Therefore, to ensure high response speed and appropriate response intensity, a new process of oxygen ashing the film surface was introduced. As a result, it was possible to secure high response intensity and high response speed at CB contents up to 30 wt%. On the basis of these results, we confirmed that CB mixing and surface oxygen ashing can improve both the response intensity and speed of sensors using metal oxide nanoparticle films.

1. Introduction

Various environmental monitoring sensors for air,⁽¹⁾ soil,⁽²⁾ water,⁽³⁾ and marine⁽⁴⁾ pollutions are required to address diverse environmental issues. Since these different environmental factors are closely interrelated, comprehensive and systematic management measures are necessary. Taking water quality sensors, which significantly affect other factors, as an example, each country establishes water quality management strategies.⁽⁵⁾ In the Republic of Korea, according to water quality management regulations, parameters such as temperature, pH,⁽⁶⁾ dissolved oxygen (BOD, COD),⁽⁷⁾ suspended solids (SS),⁽⁸⁾ total nitrogen (TN),⁽⁹⁾ and total phosphorus (TP)⁽¹⁰⁾ are continuously monitored on-site in the field.⁽¹¹⁾

However, hazardous chemicals that can have negative effects on living organisms and the environment are diverse and have small molecular sizes, making on-site monitoring difficult.

*Corresponding author: e-mail: jiho_chang@kmou.ac.kr
<https://doi.org/10.18494/SAM5007>

Therefore, periodic sampling and laboratory analysis are still being employed. Although those methods (such as spectroscopy, chromatography, and mass spectroscopy) allow for accurate analysis, it requires a time-consuming process. Considering the risk to human health or the environment caused by the rapid spreading of hazardous substances in aquatic environments, there is a need for sensor technologies that enable continuous on-site monitoring for immediate response.

Sensors capable of measuring the concentrations of hazardous chemicals in water must detect low concentrations in the water, operate at typical water temperatures, and have simple calibration and regular maintenance requirements. To address these issues, our research group proposed a sensor utilizing indium tin oxide (ITO) nanoparticles for continuous automatic measurement in water.⁽¹²⁾ We demonstrated its ability to detect oils⁽¹³⁾ and hazardous chemicals.⁽¹⁴⁾ Films using ITO nanoparticles showed a higher chemical stability in water than those using other metal oxides.⁽¹⁵⁾ Moreover, a recent result confirmed the capability of an ITO sensor to detect ethanol concentrations as low as 619 ppb.⁽¹²⁾

However, according to existing research, the measurement time was tens of minutes or more and needed improvement. One possible way to shorten the measurement time is to increase the sintering temperature to increase the conductivity of the film and minimize grain boundary scattering. This will reduce the bulk resistance of the film and also reduce the response time. In a previous study,⁽¹⁶⁾ we attempted to confirm this idea by manufacturing a sensor using an ITO film produced through sputtering. However, when the bulk resistance of the film decreased, the response intensity of the sensor decreased rapidly, so the effect of reducing the response time was unclear.

Therefore, in this study, we proposed a method of reducing the sensor response time by mixing compounds such as activated carbon (carbon black: CB). We produced an ITO:CB film and analyzed the changes in the bulk resistance, response intensity, and response time of the ITO:CB sensor.

2. Experimental Procedure

In this study, a $76 \times 26 \times 1.5 \text{ mm}^3$ quartz plate was used as the substrate, which was cleaned in distilled ionized (DI) water for 15 min in an ultrasonic bath. The ITO film was screen-printed on an area of $16 \times 13 \text{ mm}^2$, and the thickness of the printed film was $20 \pm 5 \text{ }\mu\text{m}$. ITO nanoparticles with diameters of 20–70 nm were used. The organic binder was made with a mixture of α -terpineol ($\text{C}_{10}\text{H}_{18}\text{O}$) and ethyl cellulose at a weight ratio of 19:1. Then, the ITO nanoparticles and organic binder were mixed at a weight ratio of 0.8:1 to prepare a paste with a viscosity of 550 dPa·s.

The ITO:CB film was manufactured by mixing CB and ITO while changing the weight ratio of CB (particle diameter: 35–40 nm) from 0 to 50 wt%. After printing, heat treatment was carried out at 100 °C for 3 h to remove the residual organic binder. Subsequently, O_2 ashing was performed at 225 °C for 30 min under pure O_2 gas (flow rate: 3000 sccm) to clean the surface.

To make the ITO:CB film sensor, electrodes were printed at both ends of the film using Ag paste and cured at 80 °C for 1 h. The produced ITO:CB film was compared with the ITO film

through scanning electron microscopy (SEM) and energy dispersive spectroscopy (EDS) analysis. Furthermore, electrical characteristics and changes in sensor operation were compared. Ethanol (EtOH) is a hazardous substance according to water hazard test regulations, so it was used as a representative organic solvent to monitor sensor operation. The EtOH concentration in DI water was varied from 10 to 200 ppm. To evaluate the sensor performance, we measured the change in the resistance ratio of the ITO ($\Delta R = R/R_0$, R_0 = initial resistance, R = saturation resistance). Response time was defined as the time to change from 10 to 90% of the maximum change.

3. Results and Discussion

Figure 1 shows the basic operating principle of an electrochemical sensor.⁽¹⁷⁾ As shown in Fig. 1(a), there is a difference at the interface between the chemical potential of the film (Fermi energy: E_F) and the electrochemical potential of the solution ($E[A]$). The $E[A]$ of the solution is determined using the Nernst equation. It depends on the concentration of hazardous substances in the water, which changes the space charge layer on the film surface. Therefore, when the solution concentration changes, the potential difference V_{bi} ($V_{bi} = E_F - E[A]$) changes. As a result, the surface charge concentration (n_s), which can be expressed in Eq. (1), also changes. This allows one to determine the concentration of hazardous substances in solution.

$$n_s = n_b \exp\left(-\frac{qV_{bi}}{kT}\right) \quad (1)$$

Figure 1(b) shows a schematic diagram of the ITO film. When a film composed of spherical particles of diameter D is sintered at an appropriate temperature, conductive channels are formed between the particles, promoting the transfer of charge. Here, the resistance R_{film} of the ITO film can be regarded as the parallel resistance ($R_{film} = R_S // R_B$) of the surface resistance (R_S) and the bulk resistance (R_B). Sintering the film at high temperatures improves its conductivity and

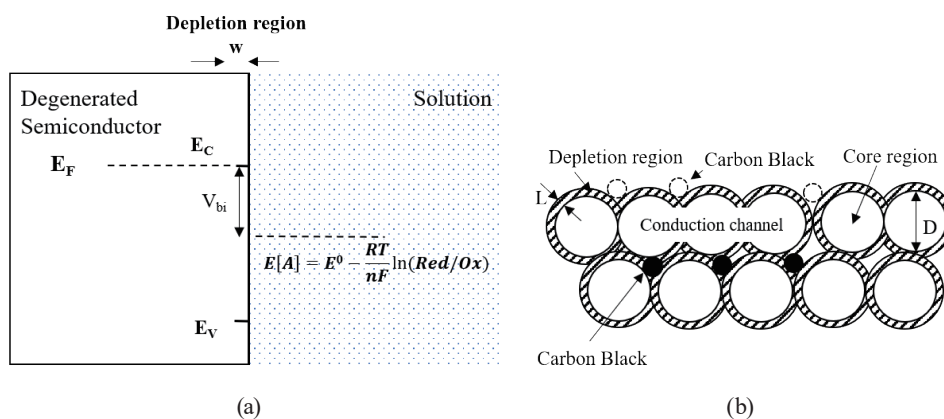


Fig. 1. Theoretical model of ITO nanoparticle film sensors. (a) Built-in potential formation at the solid and liquid interface. The electrochemical potential $E[A]$ of solution is determined using the Nernst equation. (b) Role of carbon black in the formation of conductive channels in ITO:CB films.

reduces the bulk resistance of the sensor. At this time, the sensor's response intensity ($\Delta R = R_C/R_0$) will also change, where R_C is the resistance of the film when in contact with the analyte and R_0 is the resistance before contact with the analyte. We considered the sputtered ITO film to be a suitable example with minimal bulk resistance. However, as a result of examining the characteristics of the sensor using the sputtered ITO film, we found that the response intensity of the sensor was significantly lower than that of the ITO nanoparticle film sensor.⁽¹⁶⁾ Therefore, it is necessary to look at the reason theoretically in more detail.

Figure 2 shows the relationship between the surface resistance R_S and bulk resistance R_B of the ITO film. The reference resistance R_0 of the ITO film can be expressed as a parallel resistance of R_S and R_B as shown in Eq. (2). Additionally, the resistance R_C of the sensor (contact with the analyte) can be expressed as Eq. (3). Here, δr_s and r_s represent the surface resistance of the part in contact (δr_s) and that of the part not in contact (r_s), since the diameter of the analyte droplet on the ITO surface is smaller than the distance between the electrodes. Therefore, the sensor's response ΔR can be calculated using Eq. (4).

$$R_0 = R_S // R_B = 1 / \left(\frac{1}{R_S} + \frac{1}{R_B} \right) \quad (2)$$

$$R_c \square dR_S // R_B \quad (r_s \quad \delta r_s) // R_B \quad (3)$$

$$\Delta R = \frac{R_c}{R_0} \quad (4)$$

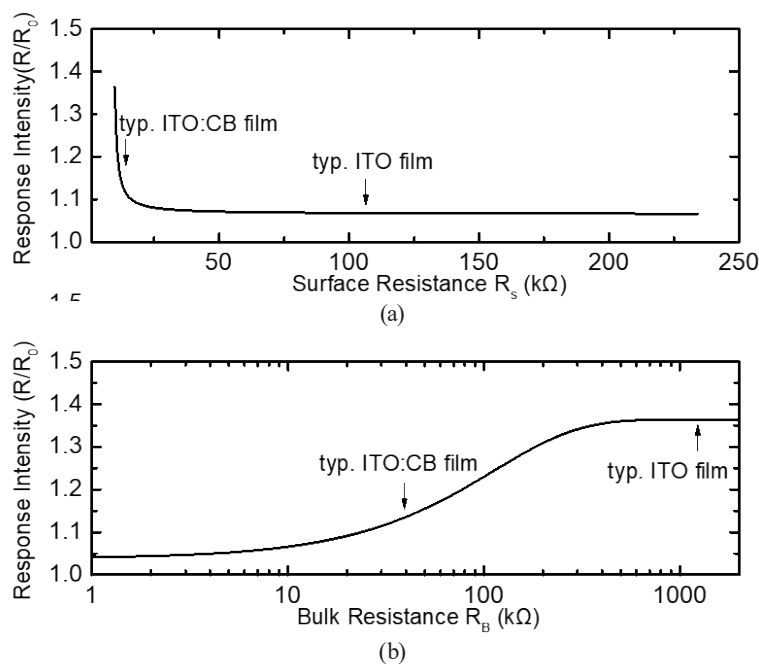


Fig. 2. Changes in sensor response intensity (ΔR) according to those in (a) surface and (b) bulk resistances of film.

As shown in Fig. 2(a), as R_S increases, the sensor response ΔR decreases, and as R_B increases, ΔR increases [Fig. 2(b)]. These calculation results clearly show that the response intensity of ITO sensors with low bulk resistance degrades rapidly.

We also show that producing films with a surface resistance that is lower than the bulk resistance is a way to produce sensors with short response times while maintaining a high response intensity. Therefore, in this study, an oxygen ashing process was introduced to remove residual contaminants and lower the surface resistance. In Fig. 2, the resistances of the typical ITO and ITO:CB films are indicated by arrows. Compared with those of the ITO film, the surface and bulk resistances of the ITO:CB film decreased. It was presumed that changes in surface resistance would increase the response strength of the sensor and those in bulk resistance would decrease the response strength of the sensor.

Figure 3 shows the selected photographic images of the ITO:CB films according to the CB content. Figure 3(a) shows the ITO film (CB, 0 wt%), whereas Figs. 3(b) to 3(f) show ITO:CB films with CB contents of (b) 1.2, (c) 2.4, (d) 4.7, (e) 33.3, and (f) 50 wt%. It is evident that as the CB mixing ratio increases, the color of the ITO:CB film darkens. EDS and SEM analyses were conducted to determine the CB contents in these samples and observe the morphological change.

Figure 4 shows the SEM images and EDS analysis data (inset) of the films. Figure 4(a) is the result for the ITO film and Fig. 4(b) is the result for the ITO:CB film. SEM images were captured

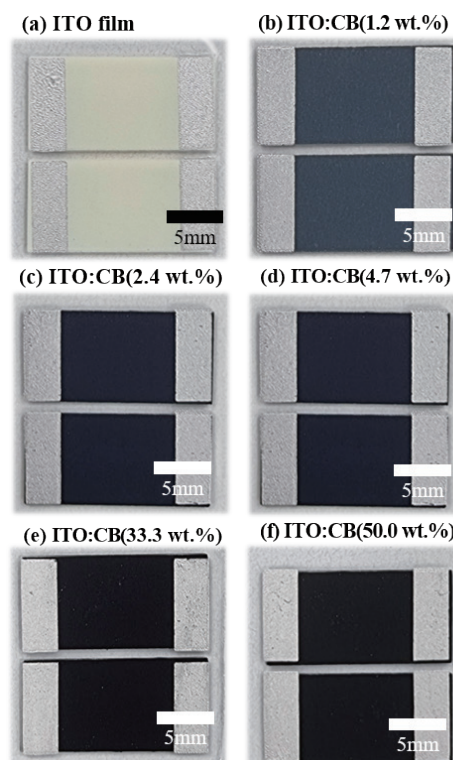


Fig. 3. (Color online) Photographs of CB-mixed ITO:CB films. (a) ITO, (b) ITO:CB (1.2 wt%), (c) ITO:CB (2.4 wt%), (d) ITO:CB (4.7 wt%), (e) ITO:CB (33.3 wt%), and (f) ITO:CB (50.0 wt%).

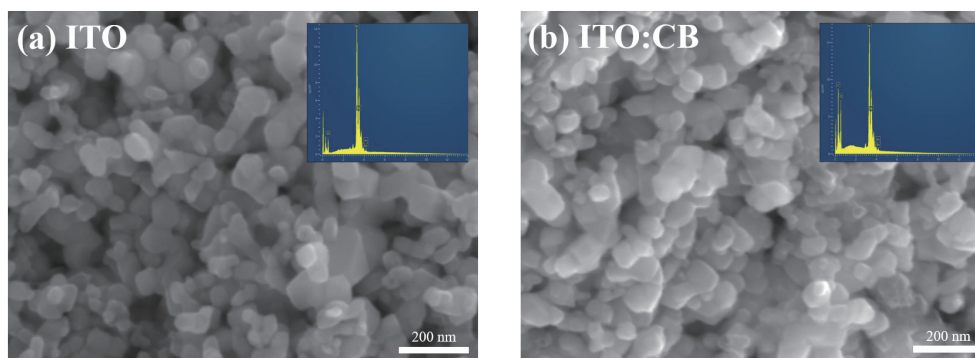


Fig. 4. (Color online) SEM and EDS measurement results (inset) of (a) ITO and (b) ITO:CB films.

at 100,000-fold magnification. No considerable morphological change was observed between the two sample surfaces. The particle size analyzed by SEM showed no significant change, with average values of 51.61 nm for the ITO film and 51.39 nm for the ITO:CB film. In the EDS analysis, the ITO film revealed the following atomic contents: In (69.7 wt%), O (20.2 wt%), Sn (5.9 wt%), and C (4.2 wt%), whereas the ITO:CB film showed the following atomic contents: In (61.7 wt%), O (21.4 wt%), C (12 wt%), and Sn (4.9 wt%). The presence of carbon in the ITO film [Fig. 4(a)] is due to the binder material, especially α -terpineol ($C_{10}H_{18}O$). Therefore, considering that value as a background effect, the total carbon content of the ITO:CB film [Fig. 3(b)] was determined to be 8.9 wt%.

Figure 5 shows the current–voltage measurement results of four selected ITO:CB samples. The inset shows the current and voltage measurement results of ITO and ITO:CB films with 1.2 and 4.5 wt% CB contents. Even a small CB content reduces the resistance significantly. For example, the ITO:CB (4.7 wt%) film exhibited a 92.24% reduction in resistance ($9.86 \times 10^3 \Omega$) compared with the ITO film ($1.27 \times 10^5 \Omega$). The resistivity also decreased from $25 \Omega\cdot\text{cm}$ for the ITO film to $10.4 \Omega\cdot\text{cm}$ for the ITO:CB film. These resistance and resistivity measurements confirmed that the addition of CB increased the conductivity.

Figure 6 shows the time-resolved sensor response observed from (a) ITO, (b) ITO:CB (1.2 wt%), (c) ITO:CB (4.7 wt%), and (d) ITO:CB (50 wt%) sensors. Measurement was performed at room temperature under 1 V external bias. After monitoring the reference response for 60 s in air, 35 μl of analyte contacted on the sensor surface. Ethanol (EtOH) was used as an analyte, which was diluted in DI water with a concentration of 10 to 200 ppm. As the CB content was increased, the response time decreased rapidly. However, a higher response intensity was only observed when the CB content was relatively low [Figs. 6(b) and 6(c)] but it decreased at the highest CB content [Fig. 6(d)].

Figure 7 shows the changes in (a) sensor response intensity (ΔR) and (b) response time (τ) according to the CB content. The sensor response was determined when the EtOH concentration was 150 ppm. As the CB content increased, both the response intensity and response time of the sensor decreased.

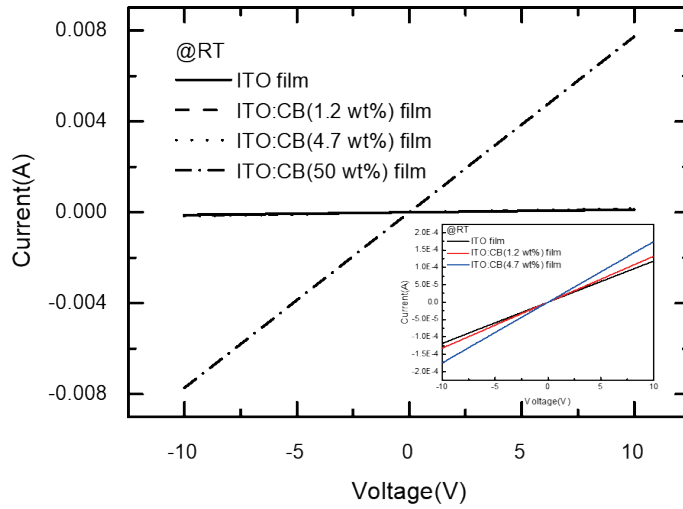


Fig. 5. (Color online) Electrical properties of ITO and ITO:CB films with various CB contents. The inset shows the I-V properties of ITO, ITO:CB (1.2 wt%), and ITO:CB (4.7 wt%) films.

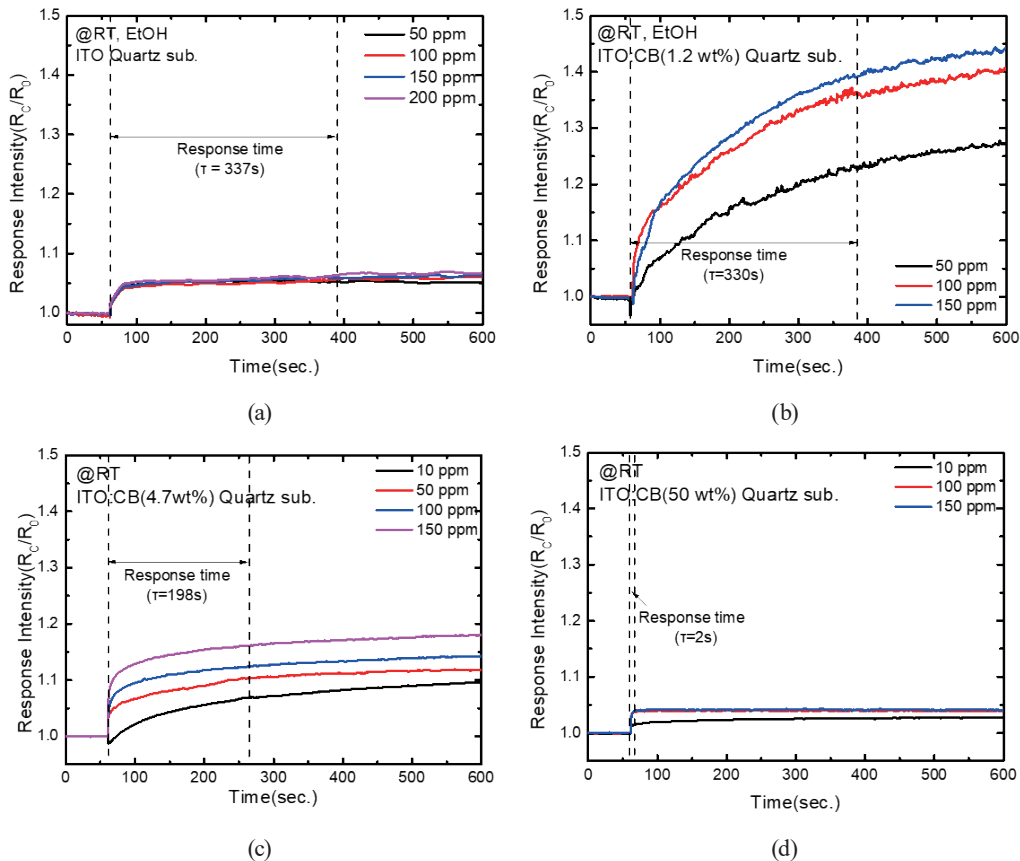


Fig. 6. (Color online) Time-resolved operating characteristics of ITO and ITO:CB sensors. (a) Response of ITO sensor. The response time is 337 s. (b) Response of ITO:CB (1.2 wt%) sensor. The response time is 330 s. (c) Response of ITO:CB (4.7 wt%) sensor. The response time is 198 s. (d) Response of ITO:CB (50 wt%) sensor. The response time is 2 s.

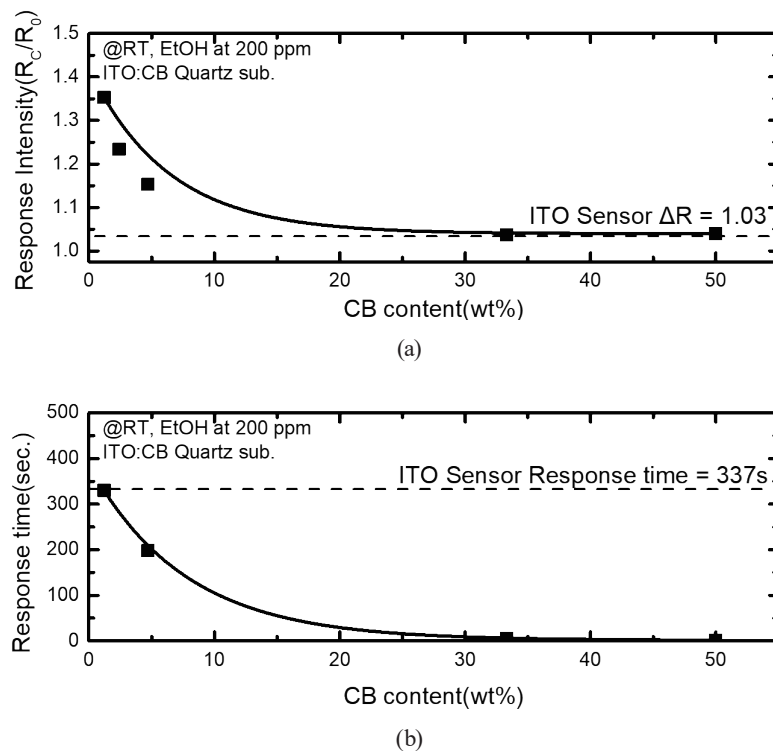


Fig. 7. Experimental results of (a) response intensity and (b) response time of ITO:CB sensors according to CB content.

This result shows that in the case of the ITO:CB sensor, as the CB content increases, the bulk resistance decreases and the response strength decreases, but a strength higher than that in the case of the ITO film sensor can be obtained at CB contents up to 30 wt%. However, the sensor's response speed continues to increase depending on the CB content. Therefore, it can be seen that relatively high response strength and speed can be secured. Additionally, these results clearly show that in the case of sensors using metal oxide nanoparticles, performance improvement cannot be achieved simply by reducing the resistance of the film by heat treatment at high temperatures. Rather, they clearly demonstrate that a method of improving conductivity and lowering the surface resistance of the film simultaneously is inevitable.

4. Conclusion

We studied ways to improve the response speed of sensors using metal oxide nanoparticles. It was shown that high response speed and improved response strength can be secured by improving conductivity by mixing CB powder and ITO nanoparticles, and reducing surface resistance through the surface treatment of an ITO:CB film. As a result, it was found that when the CB content was less than 30 wt%, the ITO:CB sensor showed a higher response intensity and a shorter response time than the ITO sensor, ensuring optimal sensor performance.

Acknowledgments

This research was supported by the Korea Institute of Marine Science & Technology Promotion (KIMST) funded by the Ministry of Oceans and Fisheries, Korea (RS-2021-KS211535).

References

- 1 H. Mayer: Atmos. Environ. **33** (1999) 24. [https://doi.org/10.1016/S1352-2310\(99\)00144-2](https://doi.org/10.1016/S1352-2310(99)00144-2)
- 2 M. L. Brusseau, I. Pepper, and C. Gerba: Environmental and Pollution Science 3rd (Elsevier, Netherlands, 2019) pp. 219–235. <https://doi.org/10.1016/C2017-0-00480-9>
- 3 W. W. Eckenfelder Jr.: Kirk-Othmer Encyclopedia of Chemical Technology (John Wiley & Sons, USA, 2000) pp. 1–29. <https://doi.org/10.1002/0471238961.1615121205031105.a01>
- 4 C. L. J. Frid and B. A. Caswell: Marine pollution (Oxford University Press, U.K, 2017).
- 5 Korea Environment Corporation, <https://www.keco.or.kr/web/lay1/S1T179C1105/contents.do> (accessed Jan. 5, 2024)
- 6 W.-D. Huang, H. Cao, S. Deb, M. Chiao, and J. C. Chiao: Sens. Actuators, A **169** (2011) 1. <https://doi.org/10.1016/j.sna.2011.05.016>
- 7 A. Kumlanghan, P. Kanatharanan, P. Asawatreratanakul, B. Mattiasson, and P. Thavarungkul: Enzyme Microb. Technol. **42** (2008) 6. <https://doi.org/10.1016/j.enzmictec.2008.01.012>
- 8 H. Ruger, M. Schwientek, B. Beckingham, B. Kuch, and P. Grathwohl: Environ. Earch Sci. **69** (2013) 373. <https://doi.org/10.1007/s12665-013-2307-1>
- 9 Y. Zhuang, W. Wen, S. Ruan, F. Zhuang, B. Xia, S. Li, H. Liu, Y. Du, and L. Zhang: Water Res. **210** (2022) 15. <https://doi.org/10.1016/j.watres.2021.117992>
- 10 H. Chem, L. Zhao, F. Yu, and Q. Du: Analyst **144** (2019) 24 <https://doi.org/10.1039/C9AN01161G>.
- 11 Korea Environment Corporation, <https://www.keco.or.kr/web/lay1/S1T179C1104/contents.do> (accessed Jan. 5, 2024).
- 12 S. S. An, C. H. Lee, J. H. Noh, Y. J. Cho, J. H. Jang, S. T. Lee, Y. M. Kim, and M. J. Lee: J. Korean Soc. Mar. Environ. **28** (2022) 23. <https://doi.org/10.7837/kosomes.2022.28.s.023>
- 13 C. H. Lee, S. S. An, Y. N. Heo, Y. J. Cho, J. H. Chang, S. T. Lee, S. W. Oh, and M. J. Lee: J. Korean Soc. Mar. Environ. **28** (2022) 30. <https://doi.org/10.7837/kosomes.2022.28.s.030>
- 14 J. S. Choi, D. W. Ko, J. Y. Seo, J. H. Nho, J. H. Chang, S. T. Lee, J. Y. Jung, and M. J. Lee: J. Korean. Phys. Soc. **76** (2020) 1005. <https://doi.org/10.3938/jkps.76.1005>
- 15 S. H. Lee, J. Y. Jung, M. J. Lee, and J. H. Jang: Sens. Mater. **29** (2017) 1. <https://doi.org/10.18494/SAM.2017.1375>
- 16 J. S. Choi: Domestic Mater's Thesis Korea Maritime and Ocean University Graduate School (2021).
- 17 M. X. Tan, P. E. Laibinis, S. T. Nguyen, J. M. Kesselman, C. E. Stanton, and N. S. Lewis: Prog. Inorg. Chem. **41** (1994) 21. <https://doi.org/10.1002/9780470166420.ch2>